Research Square

Preprints are preliminary reports that have not undergone peer review.
They should not be considered conclusive, used to inform clinical practice,
or referenced by the media as validated information.

# β-arrestin1 inhibits ferroptosis in colorectal cancer cells by modulating p53/SLC7A11 signaling

**LIFA LI**
Affiliated Hospital of North Sichuan Medical College
**JUNMO YANG**
North Sichuan Medical College
**CHENHAO ZHAO**
North Sichuan Medical College
**JINXIAO ZHANG**
Affiliated Hospital of North Sichuan Medical College
**TONG DENG**
Affiliated Hospital of North Sichuan Medical College
**SONGLIN HOU**
Affiliated Hospital of North Sichuan Medical College
**YUEHUA GUAN**
Affiliated Hospital of North Sichuan Medical College
**HE ZHOU**
zhouhe@nsmc.edu.cn
Affiliated Hospital of North Sichuan Medical College

**Research Article**

**Keywords:** colorectal cancer, ferroptosis, ARRB1, p53/SLC7A11 signaling

**Posted Date:** November 2nd, 2026

**DOI:** https://doi.org/10.21203/rs.3.rs-8048348/v1

**License:** This work is licensed under a Creative Commons Attribution 4.0 International License.
Read Full License

**Additional Declarations:**
No competing interests reported.

Table 1 is not available with this version.

# β-arrestin1 inhibits ferroptosis in colorectal cancer cells by modulating p53/SLC7A11 signaling

LIFA LI[2], JUNMO YANG[1], CHENHAO ZHAO[1],JINXIAO ZHANG[2], TONG DENG[2], SONGLIN HOU[2], YUEHUA GUAN[2],HE ZHOU[2*]

[1]Department of Clinical Medicine, North Sichuan Medical College, Nanchong, Sichuan 637000, P.R. China; [2]Department of gastrointestinal surgery, Affiliated Hospital of North Sichuan Medical College, Nanchong, Sichuan 637000, P.R. China

*Correspondence to*: Dr He Zhou, Department of gastrointestinal surgery, Affiliated Hospital of North Sichuan Medical College, Nanchong, Sichuan 637000, P.R. China
E-mail: zhouhe@nsmc.edu.cn

*Keywords*: colorectal cancer, ferroptosis, ARRB1, p53/SLC7A11 signaling

**Abstract.** Colorectal cancer (CRC) is one of the most common malignant tumors in the digestive system, and ARRB1(β-arrestin1) plays a crucial role in regulating the proliferation, invasion, migration, and other aspects of tumor cells. However, the role and regulatory mechanisms of ARRB1 in CRC have not been investigated. This study aims to investigate the molecular mechanisms by which ARRB1 affects the occurrence and development of CRC. The TCGA database was used to analyze the expression of ARRB1 in CRC. Cell proliferation, percentage of viable cells, migration, invasion, mitochondrial ferroptosis characteristics, and expression of ARRB1, p53, GPX4, and SLC7A11 were analyzed by CCK8, flow cytometry, cell cloning, scratch assay, Transwell assay, transmission electron microscopy, qRT-PCR, and Western blot, respectively. The overexpression of ARRB1 decreased the percentage of viable cells and induced cellular ROS generation in CRC cells, and the ferroptosis inducer RSL3 promoted the effects of ARRB1 overexpression on the percentage of viable cells and ROS generation. Moreover, overexpression of ARRB1 promoted CRC cell p53 nuclear

translocation, inhibited CRC cell proliferation, migration, and invasion, and decreased the levels of GPX4, GSH, and SLC7A11. However, si-TP53 inhibited the above effects of ARRB1 on cells. Up-regulation of ARRB1 promotes ferroptosis in colorectal cancer cells through p53/SLC7A11 signaling.

## Introduction

Colorectal cancer (CRC) is one of the most common malignant tumors of the digestive system, accounting for the third-highest incidence and second-highest mortality of all cancers [1]. In China, the incidence of CRC continues to increase, with approximately 550,000 new CRC patients each year, accounting for 12.2% of all new cancer diagnoses nationwide [2, 3]. Clinical treatment is mostly chosen as a combination of surgery and chemotherapy, but even among CRC patients with successfully resected tumors, tumor recurrence, and treatment resistance still exist, which seriously affects patients' efficacy, prognosis, and quality of life [4, 5]. With the development of research technology, it has become a major hotspot in CRC research to explore the mechanism of certain genes in the process of malignant progression of CRC, to screen out new specific molecular markers for early diagnosis of CRC. At the same time, selecting important molecular targets in genes and pathways and formulating individualized therapeutic plans are of significance to achieve the goal of "precision medicine" [6, 7].

ARRB1 (β-arrestin1), a member of the β-arrestins family, was initially identified as a regulator of G protein-coupled receptors (GPCRs) mediated signaling [8]. With further research, ARRB1 was found to play a crucial role in regulating cell proliferation, invasion, migration, transmitting anti-apoptotic survival signals, influencing tumor angiogenesis, and drug resistance [9-12]. Studies have shown that ARRB1 promotes gastric cancer cell proliferation, migration, and invasion, and its high expression predicts poor prognosis in gastric cancer patients [13]. Up-regulation of ARRB1 is associated with metastasis of hepatocellular carcinoma [14]. In addition, ARRB1 could lead to inhibition of hepatocyte apoptosis and up-regulation of hepatocyte compensatory proliferation [15]. However, the role and regulatory mechanisms of

ARRB1 in CRC have not been investigated.

Ferroptosis is a novel mode of programmed cell death characterized by the accumulation of lipid reactive oxygen clusters and mitochondrial crumpling [16]. It has been shown that ferroptosis inducers enhance the efficacy of radiation therapy for tumors [17]. Ferroptosis is involved in the anti-tumor effects of immune-activated CD8+T cells [18]. In addition, ferroptosis mediates endoplasmic reticulum stress, oxidative stress, and other pathways involved in disease progression [19, 20]. Studies have found that ARRB1 has the role of regulating the entry of p53 into the nucleus [21], and wild-type p53, as an important anti-tumor transcription factor, can inhibit excessive tumor proliferation by regulating the cell cycle on the one hand, and inhibit the transcription of the ferroptosis genes SLC7A11 and GPX4 on the other hand, to promote the occurrence of ferroptosis in tumor cells [22, 23]. Therefore, ARRB1 may induce ferroptosis in CRC cells by promoting the entry of wild-type p53 into the nucleus and inhibiting the expression of SLC7A11, thus exerting anti-tumor effects.

In this study, we intend to analyze the effects of ARRB1 on CRC cellular processes from the perspective of ferroptosis, to explore the molecular mechanisms by which ARRB1 regulates CRC, and to provide a theoretical basis for the use of ARRB1 as a potential diagnostic marker for cancer biology and as a drug target for CRC therapy.

## Materials and methods

*Gathering patient data.* Differential genes in CRC were screened using the TCGA database (https://cancergenome.nih.gov/), which provides clinical data on 620 patients with CRC, and correlation analyses between ARRB1 expression and cellular functional pathways (sets of functional genes) in CRC patients were performed.

*Cell culture.* Human colon cancer cells HCT116 and SW48 (iCell, Shanghai, China) were cultured in Leibovitz's L-15 medium (Procell, Wuhan, China), and the cells were digested with trypsin and then passaged after they had grown to 70%-80%.

*Cell grouping and treatment.* Setting HCT116 and SW48 cell grouping (i) pcDNA-NC + ferroptosis inducers RSL3 (0.001, 0.01, 0.1, 1, 10, 100 μM), pcDNA-ARRB1 + ferroptosis inducers RSL3 (0.001, 0.01, 0.1, 1, 10, 100 μM). (ii) pcDNA-NC, pcDNA-NC + RSL3, pcDNA-ARRB1, pcDNA-ARRB1 + RSL3. (iii) pcDNA-NC, pcDNA-ARRB1, pcDNA-ARRB1 + ferroptosis inhibitor (pcDNA-ARRB1 + Ferr-1), pcDNA-ARRB1 + autophagy inhibitor (pcDNA-ARRB1 + 3-MA), pcDNA-ARRB1 + necroptosis inhibitor (pcDNA-ARRB1 + Nec-1), pcDNA-ARRB1 + apoptosis inhibitor (pcDNA-ARRB1 + Z-VAD-FMK). (iv) pcDNA-NC + si-NC, pcDNA-NC + si-TP53, pcDNA-ARRB1 + si-NC, pcDNA-ARRB1 + si-TP53. HCT116 and SW480 cells in the logarithmic growth phase were taken, the cell density was adjusted to $2\times10^5$ cells/mL, and 2 mL/well were inoculated in 6-well plates, and cultured at 37℃ with 5% $CO_2$. The cells were transfected with overexpression plasmid (pcDNA-ARRB1, RiboBio, Guangzhou, China) and siRNA (RiboBio, Guangzhou, China) by Lipofectamine 2000 transfection reagent (Life Technologies, Shanghai, China) and riboFECT$^{TM}$CP Reagent (RiboBio, Guangzhou, China), respectively. The cells were incubated at 37℃ with 5% $CO_2$ for 6 h, and then replaced with a complete medium for further incubation. Ferr-1 (1.0 μM, MCE, USA), 3-MA (10 mM, ThermoFisher Scientific, Guangzhou, China), Nec-1 (1.0 μM, Targetmol, Shanghai, China), Z-VAD-FMK (1.0 μM, Targetmol, Shanghai, China) was used.

*CCK8 assay.* CCK8 reagent (110 μL/well, Biosharp, Shanghai, China) was added according to the assay group and incubated for 2 h. Absorbance values of each well were measured at 450 nm using an enzyme labeller (ELx800, Biotek, USA). The $IC_{50}$ was calculated.

*AnnexinV/7-AAD flow cytometry assay.* According to the grouping, cell precipitates were obtained, and after resuspending the cells with 500 μL of Binding Buffer, 5 μL of Annexin V (MULTI SCIENCES, Hangzhou, China) was added and gently blown up, and then 10 μL of 7-AAD (MULTI SCIENCES, Hangzhou, China) was added. The reaction was mixed well, and the reaction was avoided light for 5 min at room

temperature, and analyzed by flow cytometry (Cytoflex, Beckman, Beijing, China).

*Flow cytometric assay for lipid ROS.* According to the grouping, cell precipitates were obtained; the cells were resuspended uniformly in 500 μL of Lipid ROS working solution (C11-BODIPY, BioHub Biotechnology, Shanghai, China) and incubated for 30 min at 37℃ in an incubator with 5% $CO_2$. Afterward, the cells were centrifuged at 1500 r/min for 5 min, and the supernatant was aspirated and discarded. The cells were resuspended in 200 μL of PBS, and analyzed by flow cytometry (Cytoflex, Beckman, Beijing, China).

*Cell cloning assay.* After the cells of each group were cultured for 48 h, appropriate amount of medium was added to make it into cell suspension, and the cell suspension was inoculated with a density of 1,000 cells per dish into the culture medium containing 2 mL of 37℃ preheated culture solution respectively, with the cells dispersed evenly, and cultured at 37℃ and 5% $CO_2$ at a constant temperature. The culture was terminated when a single cell was observed to grow to more than 50 cell clones under the microscope. The supernatant was discarded, pure ethanol was added, fixed for 30 min, stained with 0.1% crystal violet (Bomei, Hefei, China) for 20 min, air-dried, and the images were collected, and the clones were counted.

*Scratch assay.* The cell density was adjusted to $2\times10^5$ cells/well, 2 mL/well was inoculated in 6-well plates, and when the cells grew to monolayer, the supernatant was aspirated, and the 200 μL tip was scratched perpendicular to the horizontal line behind the back to remove the scratched cells, and the cells were cultured according to the groups. 0h, 48h time points were sampled, and the cell scratch status of each well was tracked and photographed under a 50x microscope in a straight line marking place. Scratch healing distance Δd (μm) = 0h scratch width - 48h scratch width.

*Transwell assay.* 200 μL of HCT116 and SW480 cell suspension was added to the small chamber of Transwell. In the upper chamber of Transwell, 80 μL of BD matrigel

(Corning, Shanghai, China) and 4℃ pre-cooled serum-free medium (1:8) were added. The cells were incubated in 5% $CO_2$ at 37℃ for 24 h, fixed in ethanol for 30 min, and stained with 0.1% crystal violet (Bomei, Hefei, China) staining solution at room temperature for 30 min. Photographs were taken under a microscope (DMI1, LEICA, Germany), and the number of cell migrations was calculated.

*Enzyme-linked immunosorbent assay (ELISA).* The levels of glutathione peroxidase 4 (GPX4, ZC-33229, ZCiBio, Shanghai, China), glutathione (GSH, ZC-33229, ZCiBio, Shanghai, China) and Malondialdehyde (MDA, ZC-33229, ZCiBio, Shanghai, China) were detected according to the instructions of the ELISA kit.

*Transmission electron microscopy (TEM).* Cells were pre-fixed with 3% glutaraldehyde (SINOPHARM, Shanghai, China), re-fixed with 1% osmium tetroxide (Beijing Zhongjing Keyi Technology Co., Ltd.), dehydrated step by step with acetone, embedded with Epon-812 pure embedding agent, sectioned (90 nm), and stained with uranyl acetate and lead citrate (Beijing Zhongjing Keyi Technology Co., Ltd.) for 15 min and 2 min, respectively. The images of copper mesh were acquired using a JEM-1400FLASH transmission electron microscope (JEOL, Japan) was used for image acquisition of copper mesh.

*Immunofluorescence staining.* PBS washed cell crawls 3 times, dropwise addition of membrane-breaking solution (Servicebio, Wuhan, China) covered the cells and incubated at room temperature for 10 min; bovine serum was closed, and a mixture of ARRB1 primary antibody (1:100, Bioss, Beijing, China) and p53 primary antibody (1:100, Proteintech, Wuhan, China) was added and incubated at 4℃ overnight. The corresponding secondary antibody (Servicebio, Wuhan, China) was added and incubated at 37℃ for 30 min, and a drop of DAPI (Servicebio, Wuhan, China) was incubated at room temperature for 10 min, and the slices were blocked using anti-fluorescence attenuation blocker. Images were captured by digital scanning and viewing software (OlyVIA, OLYMPUS, JAPAN) and analyzed by a data image

analysis system (Image-J pro plus, National Institutes of Health, USA).

*Quantitative real-time PCR (qRT-PCR).* Cellular RNA was extracted according to Molpure® Cell/Tissue Total RNA Kit (YEASEN, Shanghai, China), reverse transcription and real-time PCR were performed according to the reagent instructions of PrimeScript RT reagent Kit (Takara, Beijing, China) and TB Green $^{TM}$ Premix Ex Taq$^{TM}$ II (Tli RNaseH Plus) (Takara, Beijing, China. GAPDH was used as the internal reference gene, and mRNA expression was calculated according to the $2^{-\Delta\Delta CT}$ method. The primer sequences are shown in Table I.

*Western blotting.* Total cellular protein was extracted from Western cell lysates, protein concentration was determined by BCA (Beyotime, Beijing, China), and 10% SDS-PAGE electrophoresis was performed, transferred to PVDF membranes, blocked with 5% skimmed milk, and incubated overnight at 4°C with primary antibodies ARRB1 (1:1000, Affinity, USA), p53 (1:1000, ABclonal, Wuhan, China), GPX4 (1:1000, ABclonal, Wuhan, China), and SLC7A11 (1:5000, ABclonal, Wuhan, China). Goat Anti-Rabbit IgG (H+L) HRP secondary antibody (1:8000, Affinity, USA) was incubated at room temperature for 2h, and the color was developed by ECL. The bands were exposed using Tanon Fluorescence Image Analysis System Software V2.0, and the exposure results were scanned by Gel-Pro analyzer4 software and expressed as the integrated optical density (IOD) of the target protein.

*Luciferase reporter assays.* Setting up the grouping, SLC7A11_LUC reporter, SLC7A11_LUC reporter + pcDNA-TP53, SLC7A11_LUC reporter + si-TP53, SLC7A11_LUC reporter + pcDNA-ARRB1, SLC7A11_LUC reporter + pcDNA-TP53 + pcDNA-ARRB1, SLC7A11_LUC reporter + si-TP53 + pcDNA-ARRB1. Prepare 293T cells for transfection, use reporter vector SLC7A11_LUC reporter, co-transfect pcDNA-TP53, si-TP53, pcDNA-ARRB1 according to the above grouping, and 48h after transfection, collect the cells and analyze them according to the Dual-Luciferase® Reporter Assay System (Promega, Madison, WI, USA) for dual-luciferase analysis.

*Statistical analysis.* All data are shown as mean ± standard deviation (SD). The SPSS 19.0 software (SPSS Inc., Chicago, USA) was used to analyze data and statistical differences between groups were determined by one way ANOVA. The LSD-*t* test was used for multiple two-by-two comparisons when the variances were equal, and Tamhane's T2 test was used when the variances were not equal. $P<0.05$ were considered statistically significant.

**Results**

*ARRB1 is lowly expressed in colorectal cancer.* Screening of CRC differential genes by TCGA data revealed that ARRB1 expression was reduced in CRC, whereas Kaplan-Meier survival analyses showed that overall survival was not improved in all ARRB1 high-expressing CRC patients ($P=0.529$, HR=0.893, Figure 1A,B) and the survival analysis of the p53 mutant subgroup showed that the overall survival rate of patients in the ARRB1 high expression and low expression groups did not differ either ($P=0.774$, HR=1.071, Figure 1C). However, in the p53 wild-type subgroup, the overall survival rate of patients with high expression of ARRB1 was higher than that of patients with low expression of ARRB1 ($P=0.0362$, HR=0.498, Figure 1D). In order to analyze the potential role of ARRB1 in CRC, the correlation between ARRB1 expression and cellular functional pathways (functional gene sets) in CRC patients was performed using the TCGA database, and we found that ARRB1 was positively correlated with gene enrichment of apoptosis pathway ($P<0.05$, ρSpearman=0.24), ferroptosis pathway ($P<0.05$, ρSpearman=0.22), and p53 signaling pathway ($P<0.05$, ρSpearman=0.10, Figure 1E), suggesting that ARRB1 may play a cancer-suppressing effect in p53 wild-type colorectal cancer.

*Effect of ARRB1 expression on ferroptosis in TP53 wild-type colorectal cancer cells.* Firstly, CCK8 was used to analyze the effect of ARRB1 on ferroptosis sensitivity of TP53 wild-type colorectal cancer cells. The results were shown in Figure 2A, the cell

viability of pcDNA-NC and pcDNA-ARRB1-treated groups decreased with the increase of RSL3 concentration ($P$<0.05). The $IC_{50}$ of RSL3 acting on pcDNA-NC and pcDNA-ARRB1 treated HCT116 cells were 4.81 and 2.06 μM, respectively, and the $IC_{50}$ acting on pcDNA-NC and pcDNA-ARRB1 treated SW48 cells were 2.86 and 5.63 μM, respectively. Subsequently, flow cytometric analysis showed that overexpression of ARRB1 decreased the percentage of viable cells and increased the ROS level. RSL3 combined with pcDNA-ARRB1 significantly decreased the percentage of viable cells and increased the ROS level when compared with the pcDNA-ARRB1 group (Figure 2B, C, D, E, $P$<0.05). In addition, combined cell death inhibitor analysis of ARRB1 on TP53 wild-type colorectal cancer, as shown in Figure 2F, G, increased the percentage of viable cells by co-treatment of pcDNA-ARRB1 with Ferr-1, 3-MA, Nec-1, and Z-VAD-FMK, respectively, as compared with the pcDNA-ARRB1 group ($P$<0.01).

*ARRB1 regulates p53 transcriptional activity to inhibit transcription of the anti-ferroptosis SLC7A11 gene.* Here, we analyzed the effect of ARRB1 on p53 nuclear translocation, as shown in Figure 3A, the expression of p53 in the nucleus of HCT116 and SW48 cells was significantly increased after treatment with pcDNA-ARRB1 compared with the pcDNA-NC group ($P$<0.01). As shown in Figure 3B, luciferase reporter assay was performed to analyze the effect of ARRB1 expression on the transcriptional activity of p53 downstream of the anti- ferroptosis SLC7A11 promoter, compared with the SLC7A11_LUC reporter + pcDNA-ARRB1 group, the fluorescence activity of the SLC7A11_LUC reporter + pcDNA-ARRB1+ pcDNA-TP53 group was significantly reduced, while the fluorescence activity of SLC7A11_LUC reporter + pcDNA-ARRB1 + si-TP53 group was significantly higher ($P$<0.01). Furthermore, immunofluorescence staining showed that the positive cell counts of ARRB1 with p53 increased after pcDNA-ARRB1 treated cells ($P$<0.01).

*ARRB1 depends on p53 to induce ferroptosis in TP53 wild-type colorectal cancer cells.* In this part, we first examined the cell proliferation and migration ability. The results showed that compared with the pcDNA-NC + si-NC group, the pcDNA-NC + si-TP53

group significantly increased cell proliferation (Figure 4A, B), cell migration (Figure 4C, D), cell invasion (Figure 4E, F), and cell viability ratio (Figure 4G, H). However, the pcDNA-ARRB1 + si-NC group showed an opposite effect to the pcDNA-NC + si-TP53 group ($P$<0.05). Compared with the pcDNA-ARRB1 + si-NC group, si-TP53 reversed the effect of pcDNA-ARRB1 on the cells ($P$<0.01).

Also, compared with the pcDNA-NC + si-NC group, the pcDNA-ARRB1 + si-NC group significantly increased the level of cellular ROS (Figure 5A, B), elevated the MDA activity, but significantly attenuated the activities of GPX4 and GSH (Figure 4C, $P$<0.05). However, si-TP53 reversed the above effects of pcDNA-ARRB1 on cells ($P$<0.05). Transmission electron microscopy results showed that the mitochondria of the pcDNA-NC + si-NC group and pcDNA-NC + si-TP53 group had a more normal morphology and structure and the cell membrane was intact and continuous. In the pcDNA-ARRB1 + si-NC group, mitochondria were crumpled and some cell membranes were broken. In the pcDNA-ARRB1 + si-TP53 group, mitochondria were mildly crumpled and there was no obvious abnormality in the cell membrane (Figure 5D). Moreover, compared with the pcDNA-NC + si-NC group, the pcDNA-ARRB1 + si-NC group significantly increased the mRNA and protein expression of ARRB1 and p53, and significantly decreased the mRNA and protein expression of GPX4 and SLC7A11. But si-TP53 reversed the above effects of pcDNA-ARRB1 on the cells (Figure 5E, F, G, $P$<0.05).

**Discussions**

In this study, overexpression of ARRB1 decreased the percentage of viable cells and induced cellular ROS generation in CRC cells, and the ferroptosis inducer RSL3 promoted the effects of ARRB1 overexpression on the percentage of viable cells and ROS generation. Moreover, overexpression of ARRB1 promoted CRC cell p53 nuclear translocation, inhibited CRC cell proliferation, migration, and invasion, and decreased the levels of GPX4, GSH, and SLC7A11. However, si-TP53 inhibited the above effects of ARRB1 on cells.

Biological behaviors such as proliferation, migration, and invasion of malignant tumors are regulated by multiple molecules and signals [24]. As a scaffolding protein,

β-arrestins regulate multiple signaling pathways, thereby influencing biological behaviors such as cell survival, proliferation, and migration [25]. ARRB1, a member of the β-arrestins family, has been shown to regulate multiple intracellular signaling networks [26]. Researchers have found that overexpressing ARRB1 increases p-AKT and p-ERK1/2 expression in gastric cancer N87 cells, through the AKT/ERK signaling pathway, ARRB1 up-regulation correlated with poor prognosis and promoted metastasis and epithelial-mesenchymal transition in gastric cancer [13]. Additionally, ARRB1 knockdown inhibited pancreatic cancer cell proliferation and migration, blocked cancer cells in the G0/G1 phase, and promoted apoptosis [11]. In CRC, ARRB1 can increase cell survival and inhibit apoptosis [27]. This study found that overexpression of ARRB1 inhibited cell proliferation, migration, and invasion, ARRB1 may have an oncogenic effect in p53 wild-type CRC cells.

MDA is the most prevalent by-product of lipid peroxidation and is defined as a marker of ferroptosis [28]. Also, the cytotoxicity of ferroptosis is dependent on the production of ROS [29]. Depletion of GSH is also a key ferroptosis marker [30]. The central mechanism of ferroptosis is the accumulation of lipid peroxidation, which is driven by lipid peroxidation that is usually triggered by inhibition of SLC7A11 and GPX4, with reduced SLC7A11 expression leading to a shortage of GSH [31]. Inhibition of GPX4 impairs the ability to neutralize lipid peroxides via GSH [32]. Cancer cells can protect themselves from ferroptosis by promoting their antioxidant system [33]. In this experiment, up-regulation of ARRB1 induced ROS production in CRC cells and decreased the levels of GPX4, GSH, and SLC7A11. The ferroptosis inducer RSL3 promotes the effect of ARRB1 overexpression on ROS production. This suggests that up-regulation of ARRB1 leads to an increase in lipid peroxidation and ultimately induces ferroptosis in CRC cells.

Studies have reported that the oncogene p53 can enhance ferroptosis by inhibiting the expression of SLC7A11 [34]. In this experiment, we found that overexpression of ARRB1 promoted nuclear translocation of p53 in CRC cells, which is consistent with the results of cancer cell growth inhibition. It is also noted herein that si-TP53 inhibited the effect of ARRB1 up-regulation on the reduction of cellular GPX4, GSH, and

SLC7A1, and that GSH was inhibited by p53, which may sensitize the cells to ferroptosis by inhibiting SLC7A11 and promoting ROS production. In addition, different types of inhibitors (Fer-1, 3-MA, Nec-1, Z-VAD-FMK) were used in this experiment to act on CRC cells overexpressing ARRB1, and the above inhibitors significantly reversed the effect of up-regulation of ARRB1 on the reduction of the percentage of viable cells. This further suggests that ARRB1 reduces the percentage of live cells in CRC possibly by inducing a new programmed cell death- ferroptosis, and regulating the p53/SLC7A11 axis to induce cellular ferroptosis.

In conclusion, we found that overexpression of ARRB1 inhibited the proliferation, migration, and invasion of CRC cells and decreased the levels of ferroptosis markers GPX4, GSH, and SLC7A11. Si-TP53 reversed the above effects of ARRB1 on cells. These findings suggest that up-regulation of ARRB1 promotes ferroptosis in CRC cells by regulating p53/SLC7A11 signaling.

**Acknowledgements**

Not applicable.

**Funding**

The present study was supported by the Youth Foundation of North Sichuan Medical College (CBY23-QNA43).

**Availability of data and materials**

The data generated in the present study may be requested from the corresponding author.

**Authors' contributions**

ZH, LL and CZ designed the study. LL, CZ, JZ, YG, RY, and SH performed the majority of the experiments. ZH, LL and CZ analyzed the data. JZ, YG, RY, SH and ZT provided assistance for the experiments and data analysis. ZH, LL and CZ wrote the draft of the manuscript. ZH revised the manuscript. ZH, LL and CZ confirm the authenticity of all the raw data. All authors have read and approved the final manuscript.

**Ethics approval and consent to participate**

Not applicable.

**Patient consent for publication**

Not applicable.

**Competing interests**

The authors declare that they have no competing interests.

**References**


1. Morgan E, Arnold M. Global burden of colorectal cancer in 2020 and 2040: incidence and mortality estimates from GLOBOCAN. Gut. 2023 Feb;72(2):338-44.
2. Xia C, Dong X, Li H, Cao M, Sun D, He S, et al. Cancer statistics in China and United States, 2022: profiles, trends, and determinants. Chinese medical journal. 2022 Feb 9;135(5):584-90.
3. Wang Z, Dan W, Zhang N, Fang J, Yang Y. Colorectal cancer and gut microbiota studies in China. Gut microbes. 2023 Jan-Dec;15(1):2236364.
4. Cervantes A, Adam R, Roselló S, Arnold D, Normanno N, Taïeb J, et al. Metastatic colorectal cancer: ESMO Clinical Practice Guideline for diagnosis, treatment and follow-up. Annals of oncology : official journal of the European Society for Medical Oncology. 2023 Jan;34(1):10-32.
5. Leowattana W, Leowattana P, Leowattana T. Systemic treatment for metastatic colorectal cancer. World journal of gastroenterology. 2023 Mar 14;29(10):1569-88.
6. Ciardiello F, Ciardiello D, Martini G, Napolitano S, Tabernero J, Cervantes A. Clinical management of metastatic colorectal cancer in the era of precision medicine. CA: a cancer journal for clinicians. 2022 Jul;72(4):372-401.
7. Bao Y, Zhai J, Chen H. Targeting m(6)A reader YTHDF1 augments antitumour immunity and boosts anti-PD-1 efficacy in colorectal cancer. Gut. 2023 Aug; 72(8): 1497-509.
8. Luo Y, Lei Y, Zhou H, Chen Y, Liu H, Jiang J, et al. ARRB1 downregulates acetaminophen-induced hepatoxicity through binding to p-eIF2α to inhibit ER stress signaling. Cell biology and toxicology. 2024 Jan 22;40(1):1.

9. Sunitha J, Mahendra J, Mahendra L, Devaraj N. Molecular docking studies of a-mangostin with oral cancer targets ARRB1, FLNA, CALM3 and HTT. Bioinformation. 2020;16(8):625-30.
10. Lei Y, Xu X, Liu H, Chen L, Zhou H, Jiang J, et al. HBx induces hepatocellular carcinogenesis through ARRB1-mediated autophagy to drive the G(1)/S cycle. Autophagy. 2021 Dec;17(12):4423-41.
11. Zhang X, Kong Z, Xu X, Yun X, Chao J, Ding D, et al. ARRB1 Drives Gallbladder Cancer Progression by Facilitating TAK1/MAPK Signaling Activation. Journal of Cancer. 2021;12(7):1926-35.
12. Ye Y, Jiang H, Wu Y, Wang G, Huang Y, Sun W, et al. Role of ARRB1 in prognosis and immunotherapy: A Pan-Cancer analysis. Frontiers in molecular biosciences. 2022;9:1001225.
13. Yu H, Wang M, Zhang T, Cao L, Li Z, Du Y. Dual roles of β-arrestin 1 in mediating cell metabolism and proliferation in gastric cancer. Proceedings of the national academy of sciences of the united states of america. 2022 Oct 4;119(40): e2123231119.
14. Xu X, Lei Y. β-Arrestin1 is involved in hepatocellular carcinoma metastasis via extracellular signal-regulated kinase-mediated epithelial-mesenchymal transition. Journal of gastroenterology and hepatology. 2020 Dec;35(12):2229-40.
15. Qi Z, Qi S, Gui L, Shen L. β-arrestin2 regulates TRAIL-induced HepG2 cell apoptosis via the Src-extracellular signal-regulated signaling pathway. Molecular medicine reports. 2016 Jul;14(1):263-70.
16. Jiang X, Stockwell BR. Ferroptosis: mechanisms, biology and role in disease. Nature reviews molecular cell biology. 2021 Apr;22(4):266-82.
17. Lei G, Zhang Y. The role of ferroptosis in ionizing radiation-induced cell death and tumor suppression. Cell research. 2020 Feb;30(2):146-62.
18. Liao P, Wang W, Wang W, Kryczek I, Li X, Bian Y, et al. CD8(+) T cells and fatty acids orchestrate tumor ferroptosis and immunity via ACSL4. Cancer cell. 2022 Apr 11;40(4):365-78.e6.

19. Liu Z, Nan P, Gong Y, Tian L, Zheng Y, Wu Z. Endoplasmic reticulum stress-triggered ferroptosis via the XBP1-Hrd1-Nrf2 pathway induces EMT progression in diabetic nephropathy. Biomedicine & pharmacotherapy = Biomedecine & pharmacotherapie. 2023 Aug;164:114897.
20. Li Y, Li M, Feng S, Xu Q, Zhang X, Xiong X, et al. Ferroptosis and endoplasmic reticulum stress in ischemic stroke. Neural Regen Res. 2024 Mar;19(3):611-18.
21. Tocci P, Cianfrocca R, Di Castro V, Rosanò L, Sacconi A, Donzelli S, et al. β-arrestin1/YAP/mutant p53 complexes orchestrate the endothelin A receptor signaling in high-grade serous ovarian cancer. Nature communications. 2019 Jul 19; 10(1):3196.
22. Jiang L, Kon N, Li T, Wang SJ, Su T, Hibshoosh H, et al. Ferroptosis as a p53-mediated activity during tumour suppression. Nature. 2015 Apr 2;520(7545):57-62.
23. Kang R, Kroemer G, Tang D. The tumor suppressor protein p53 and the ferroptosis network. Free radical biology & medicine. 2019 Mar;133:162-68.
24. Ullah R, Yin Q, Snell AH, Wan L. RAF-MEK-ERK pathway in cancer evolution and treatment. Seminars in cancer biology. 2022 Oct;85:123-54.
25. Aamna B, Kumar Dan A. Deciphering the signaling mechanisms of β-arrestin1 and β-arrestin2 in regulation of cancer cell cycle and metastasis. Journal of cellular physiology. 2022 Oct;237(10):3717-33.
26. Shu Y, Wang Y, Lv WQ, Peng DY, Li J, Zhang H, et al. ARRB1-Promoted NOTCH1 Degradation Is Suppressed by OncomiR miR-223 in T-cell Acute Lymphoblastic Leukemia. Cancer research. 2020 Mar 1;80(5):988-98.
27. Zhang Z, Zhong X, Xiao Y, Chen C. MicroRNA-296 inhibits colorectal cancer cell growth and enhances apoptosis by targeting ARRB1-mediated AKT activation. Oncology reports. 2019 Jan;41(1):619-29.
28. Wen RJ, Dong X, Zhuang HW, Pang FX, Ding SC, Li N, et al. Baicalin induces ferroptosis in osteosarcomas through a novel Nrf2/xCT/GPX4 regulatory axis. Phytomedicine : international journal of phytotherapy and phytopharmacology. 2023 Jul 25;116:154881.

29. Park E, Chung SW. ROS-mediated autophagy increases intracellular iron levels and ferroptosis by ferritin and transferrin receptor regulation. Cell death & disease. 2019 Oct 28;10(11):822.

30. Ursini F, Maiorino M. Lipid peroxidation and ferroptosis: The role of GSH and GPx4. Free radical biology & medicine. 2020 May 20;152:175-85.

31. Fu C, Wu Y, Liu S, Luo C, Lu Y, Liu M, et al. Rehmannioside A improves cognitive impairment and alleviates ferroptosis via activating PI3K/AKT/Nrf2 and SLC7A11/GPX4 signaling pathway after ischemia. Journal of ethnopharmacology. 2022 May 10;289:115021.

32. Zeng C, Lin J, Zhang K, Ou H, Shen K, Liu Q, et al. SHARPIN promotes cell proliferation of cholangiocarcinoma and inhibits ferroptosis via p53/SLC7A11/GPX4 signaling. Cancer Science. 2022 Nov;113(11):3766-75.

33. Chen Q, Zheng W, Guan J, Liu H, Dan Y, Zhu L, et al. SOCS2-enhanced ubiquitination of SLC7A11 promotes ferroptosis and radiosensitization in hepatocellular carcinoma. Cell death and differentiation. 2023 Jan;30(1):137-51.

34. Guan Z, Chen J, Li X, Dong N. Tanshinone IIA induces ferroptosis in gastric cancer cells through p53-mediated SLC7A11 down-regulation. Bioscience reports. 2020 Aug 28;40(8).

**Figure**

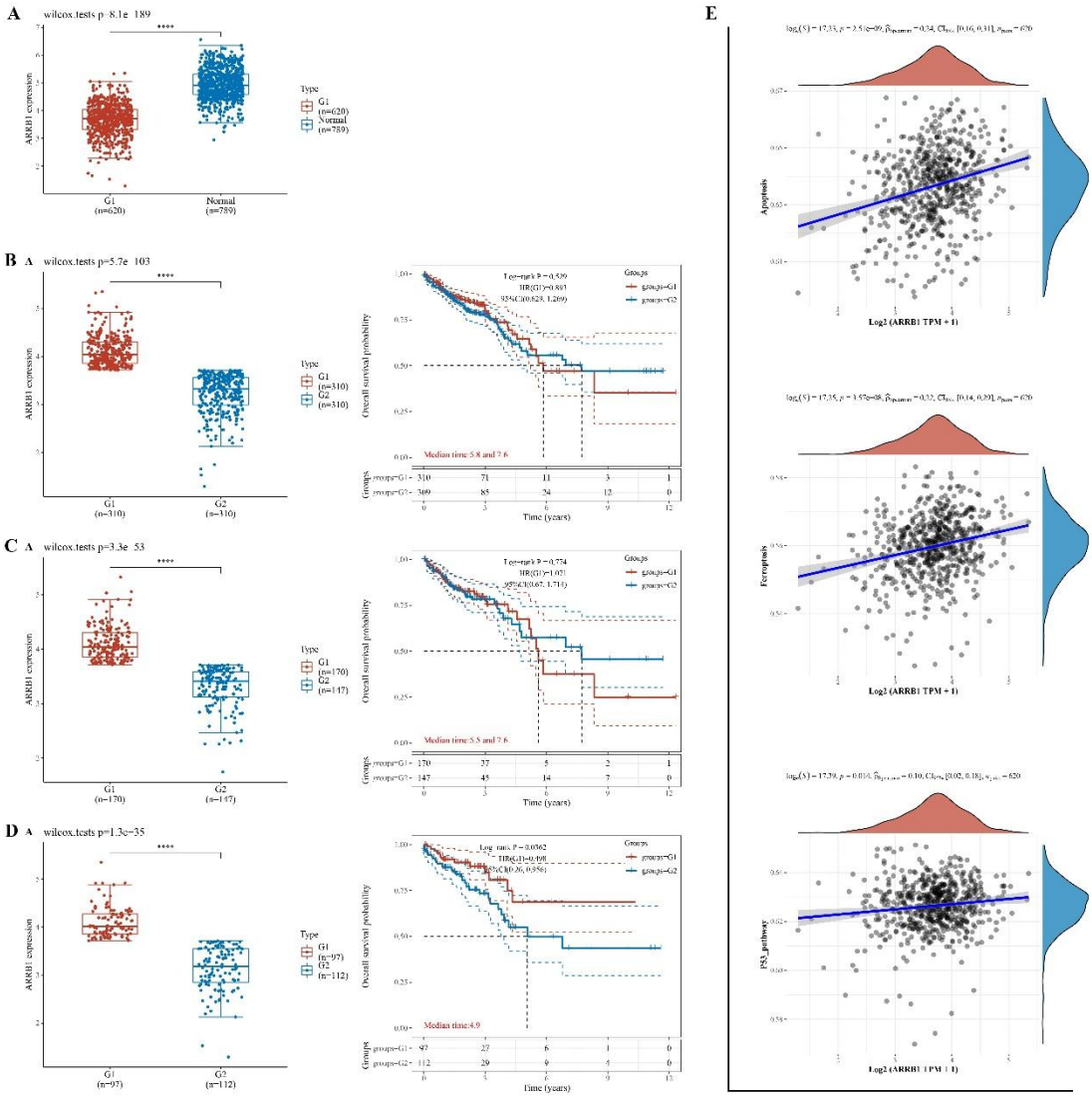



**Figure1** ARRB1 is lowly expressed in colorectal cancer. A: The expression of ARRB1 in CRC was analyzed using the TCGA database. B: Overall survival analysis of CRC patients with high ARRB1 expression. C: Overall survival analysis of patients with high versus low ARRB1 expression in the p53 mutant subgroup. D: Overall survival analysis of patients with high versus low ARRB1 expression in the p53 wild-type subgroup. E: Correlation analysis of ARRB1 expression with cellular functional pathways (functional gene sets).

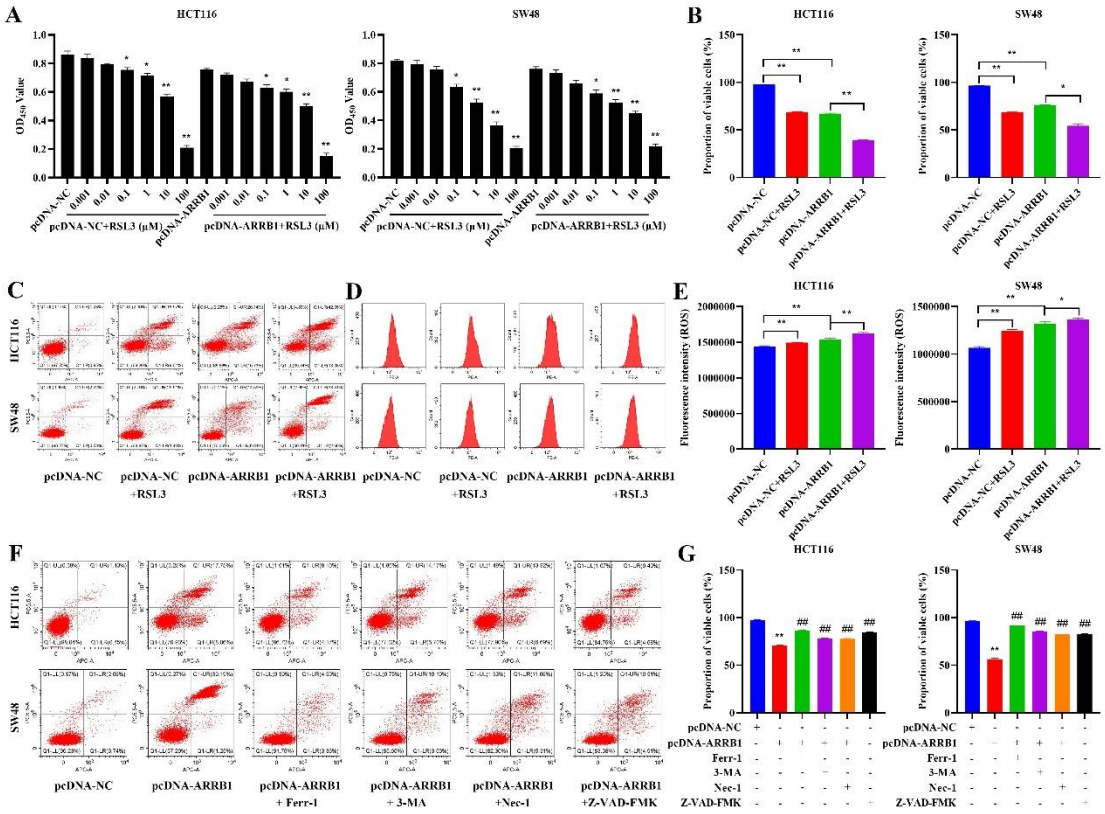



**Figure2** Effect of ARRB1 expression on ferroptosis in TP53 wild-type colorectal cancer cells. A: Cell viability. B: Percentage of viable cells. C: Representative flow cytometric plot of percentage of live cells. D: Flow cytometric representation of ROS. E: Levels of ROS in cells. F: Representative flow cytometric plot of percentage of live cells. G: Percentage of viable cells. Data expressed as mean ± SD. Compared with pcDNA-NC group, **P*<0.05, ***P*<0.01, Compared with pcDNA-ARRB1 group, ##*P*<0.01.

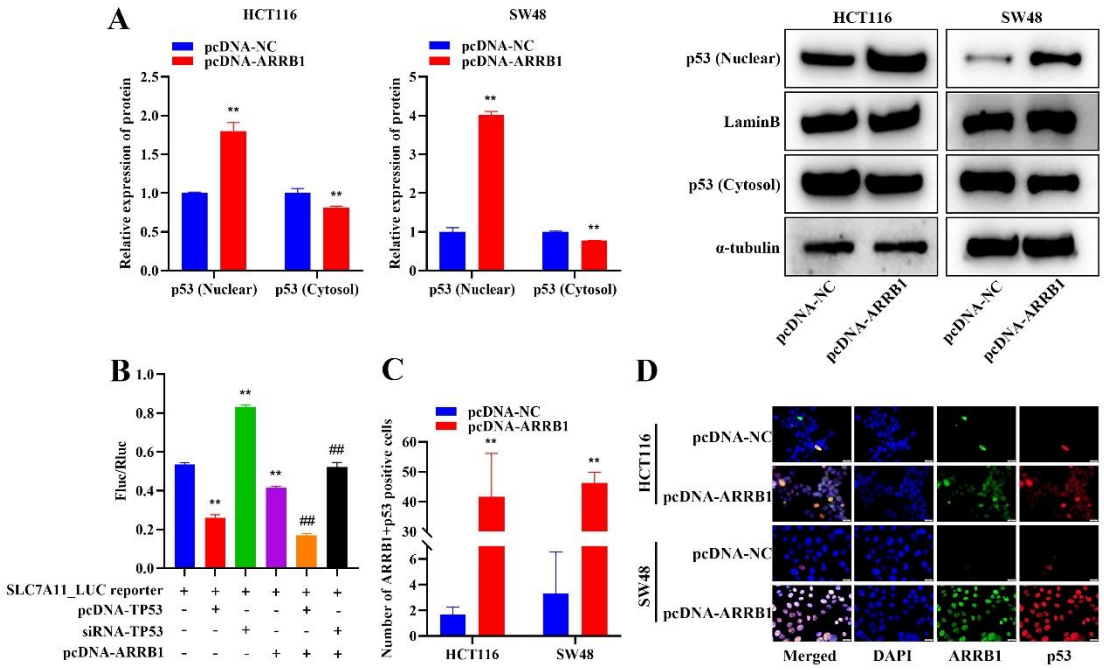



**Figure3** ARRB1 regulates p53 transcriptional activity to inhibit transcription of the anti- ferroptosis SLC7A11 gene. A: Western blot to detect the expression of nuclear p53, cytoplasmic p53. B: Transcriptional activity of the SLC7A11 promoter was analyzed by luciferase reporter assay. C: Immunofluorescence overview of co-localization and nuclear translocation of ARRB1 and p53. Data expressed as mean ± SD. Compared with pcDNA-NC or SLC7A11_LUC reporter group, ***P*<0.01, Compared with SLC7A11_LUC reporter + pcDNA-TP53 or SLC7A11_LUC reporter +si-TP53 group, ##*P*<0.01.

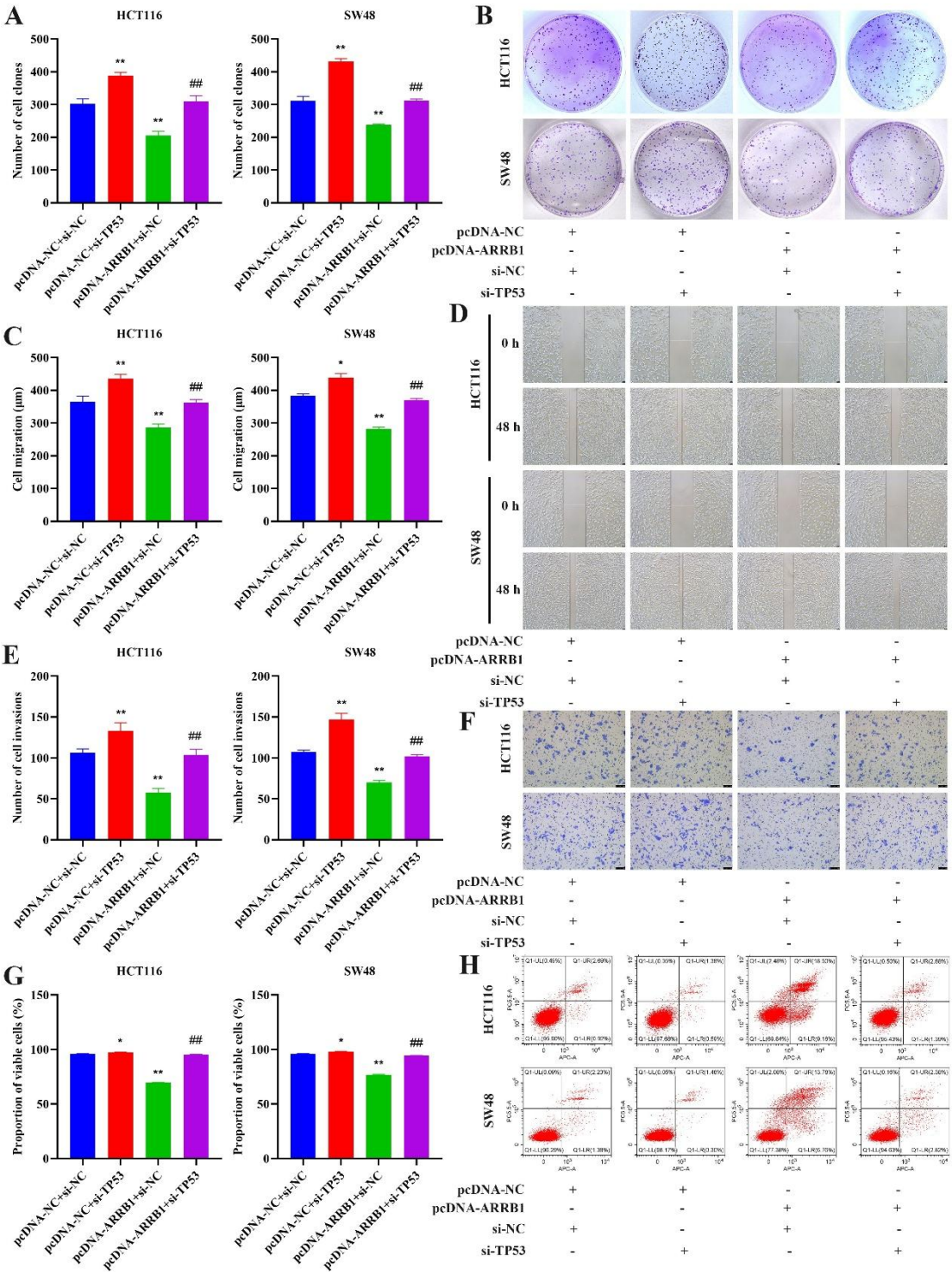



**Figure4** ARRB1 depends on p53 to induce ferroptosis in TP53 wild-type colorectal cancer cells. A: Number of cell clones. B: Representative images of cell clones (crystal violet staining). C: Cell migration. D: Representative pictures of cell migration (Bar: 250 μm). E: Cell migration. F: Representative pictures of cell migration (crystal violet staining, Bar: 100 μm). G: Percentage of viable cells. H: Representative flow cytometric

plot of percentage of live cells. Data expressed as mean ± SD. Compared with pcDNA-NC + si-NC group, **P*<0.05, ***P*<0.01, Compared with pcDNA-ARRB1 + si-NC group, ##*P*<0.01.

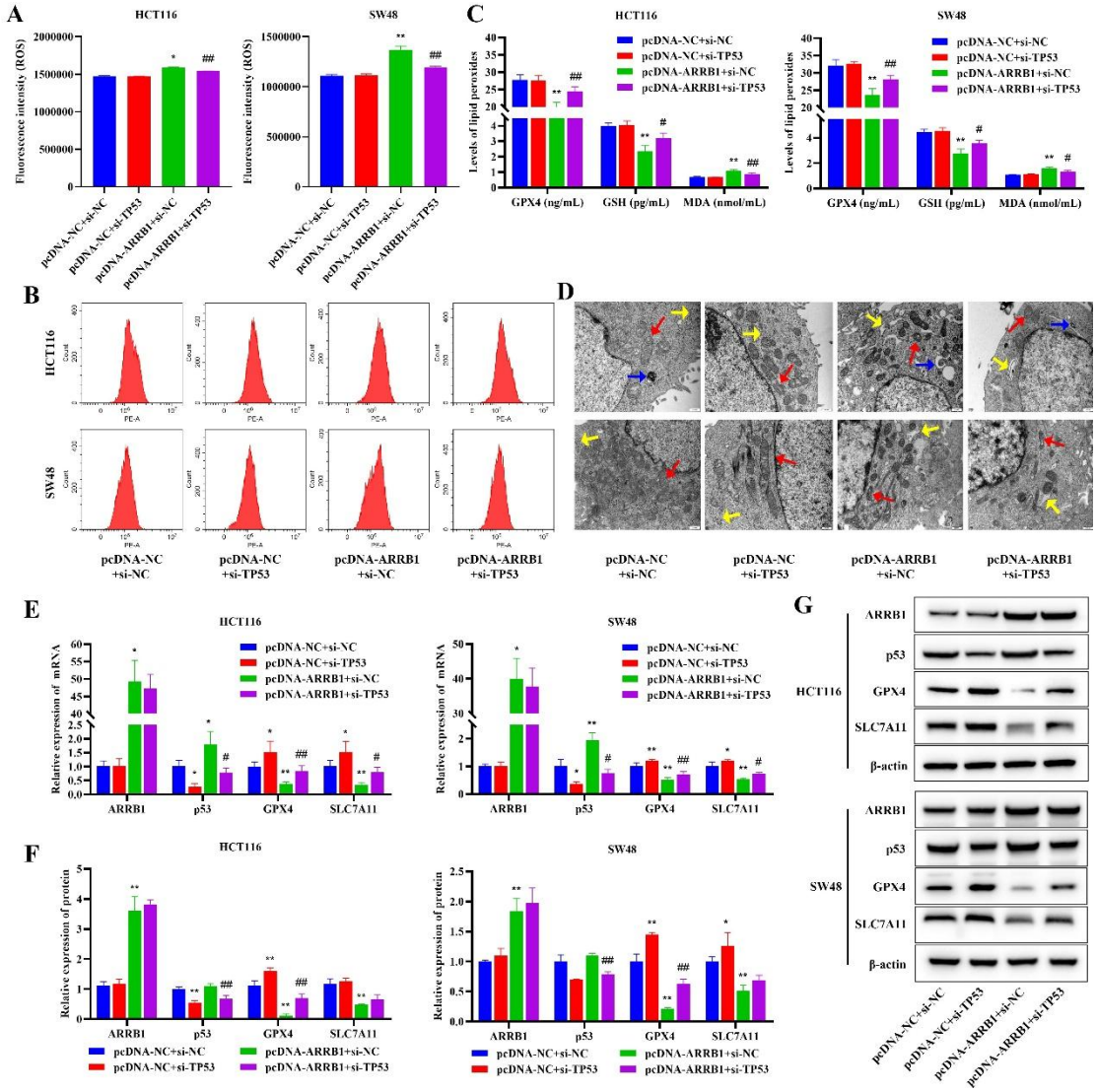



**Figure5** ARRB1 depends on p53 to induce ferroptosis in TP53 wild-type colorectal cancer cells. A: Levels of ROS in cells. B: Representative flow cytometric plot of percentage of live cells. C: Cellular levels of GPX4, GSH, and MDA. D: Changes in cellular mitochondrial iron death characteristics were observed by transmission electron microscopy (20000, Bar: 500 nm, red arrows: normal mitochondria or wrinkled mitochondria; yellow arrows: normal rough endoplasmic reticulum or dilated rough endoplasmic reticulum; blue arrows: autophagy). E: The expression of ARRB1, p53, GPX4, and SLC7A11 in cells was analyzed by qRT-PCR. F-G: Western blot

analyzed the protein expression of ARRB1, p53, GPX4, and SLC7A11 in the cells. Data expressed as mean ± SD. Compared with pcDNA-NC + si-NC group, **P*<0.05, ***P*<0.01, Compared with pcDNA-ARRB1 + si-NC group, #*P*<0.05, ##*P*<0.01.